NUMERICAL METHOD FOR SHOCK FRONT HUGONIOT STATES

J. M. D. Lane* **and M. Marder***

**Center for Nonlinear Dynamics, University of Texas at Austin*

Abstract. We describe a Continuous Hugoniot Method for the efficient simulation of shock wave fronts. This approach achieves significantly improved efficiency when the generation of a tightly spaced collection of individual steady-state shock front states is desired, and allows for the study of shocks as a function of a continuous shock strength parameter, v_p. This is, to our knowledge, the first attempt to map the Hugoniot continuously. We apply the method to shock waves in Lennard-Jonesium along the $<100>$ direction. We obtain very good agreement with prior simulations, as well as our own benchmark comparison runs.
Keywords: Shock waves, Molecular dynamics, Hugoniot, Lennard-Jones potentials
PACS: 52.35.Tc, 62.50.+p, 31.15.Qg

INTRODUCTION

On-going experiments the University of Texas at Austin are investigating the shock-strength dependence of melt time scales in tin using terawatt laser systems on sub-picosecond time scales. Large numbers of trials exploring many different shock velocities will be possible. We present here a method intended to provide direct comparisons with these experiments.

There are two major difficulties with applying traditional simulation methods [1] [2] [3] to the study of the dynamics near the shock front: (1) To produce the environment at the front, one must simulate a large and ever-growing system, of which the front constitutes only a very small fraction; and (2) The conditions within a steady-state shock take long times to arise, and each computationally-expensive shock run results in only a single data point.

The constrained dynamics methods of the Hugoniostat and others [4] [5] offer a solution to the first issue, but provide no information about non-equilibrium dynamics at the shock front that would be needed to compare with experiments. The approach of Zhakhovskii et al. [6] succeeds in addressing the first point at the shock front, but does not address the second. We generalize and expand on their methods. First, we concentrate our efforts on the neighborhood of the shock interface, thereby increasing computational efficiency, and second, we map system response to a continuum of shock strength final states in a single run. These, combined, constitute the Continuous Hugoniot Method.

CONTINUOUS HUGONIOT METHOD

Our simulation method makes the Hugoniot the thermodynamic path of our simulation system. This has not been possible experimentally. Figure 1 contrasts the experimental loading paths (Rayleigh lines) to each state of the Hugoniot and the loading path which we will use to reach the same state points.

We outline our simulation method in four stages:
Benchmark – We begin each simulation with a traditional shock wave computation. This initial long duration, full-system run is allowed to continue to its final shock steady state. This steady state is our first point on the shock Hugoniot and serves to seed our subsequent computations. In Figure 1 this is represented by the lower Rayleigh line from the initial state to the beginning of the Hugoniot ramp.
Reduce – We truncate the system to a fixed width neighborhood around the front by removing parti-

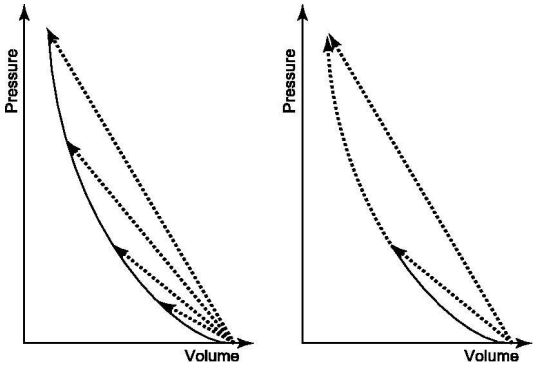

FIGURE 1. (left) The Hugoniot, as a collection of final shock states; and (right) as the state-to-state path of the Continuous Hugoniot Method.

cles which are beyond a set distance behind the shock front. We impose a warm impactor (piston) boundary condition and match the thermodynamic statistics at the rear purge point using a strong Langevin thermostat. A buffer of pristine material is preserved ahead. The length of the reduced system is determined by the system's thermalization length. The piston driving velocity and mean velocity of the thermostat are equal, and this value, v_p, serves as the external control parameter for shock strength.

Shock strength ramp – To this reduced system, we introduce a quasistatic increase of the shock forcing parameter. The goal is to increase the shock strength, while always maintaining a direct mechanical coupling between the forcing at the piston and the response at the shock interface. The piston velocity increases by a set amount per timestep. The temperature of the stochastic forcing is updated every purge to match the distribution at the purge point. The point of forcing always remains a set distance behind the shock front. This process continues until the shock strength parameter has reached its terminal value.

Terminal benchmark comparison – Finally, a second benchmark run is made with a shock strength matched to the final value of the shock strength ramp. This allows the final state of the Hugoniot ramp to be compared directly to a traditional shock run to identify any problems and to serve as an error check.

Validity of Shock States

The validity of our purge technique assumes that the back of our system is in equilibrium. We verify this by velocity distribution analysis before we reduce the system. We assume our shocks are always in steady state. This is guaranteed, so long as our ramp loading is quasistatic. If so, the small changes have time to equilibrate across the entire system and the driving and response are mechanically coupled. If not, then the foundation of the Hugoniot-Rankine equations is eroded, and off-Hugoniot states are produced.

The essential property of this method is our ability to very slowly ramp the shock strength parameter while maintaining correct thermodynamic conditions at a roughly constant distance behind the front. This is not currently achievable in experiment. Instead, in experiments driving forces are imposed at ever-increasing distances. If one ramps the driving velocity in an experimental situation, the result is isentropic compression rather than a shock response.

Velocity Ramp Rate

We can estimate an upper bound for the quasistatic ramp rate of the shock strength control parameter. The velocity is scaled by units of the wave speed of the compressed material, C_S, and the time is scaled by the return time of the acoustic waves in the system, $2L/C_S$. We, thus, get the nondimensional condition for a quasistatic ramp.

$$\dot{\tilde{v}}_p = \frac{d\tilde{v}_p}{d\tilde{t}} = \frac{d(v_p/C_S)}{d(t/\frac{2L}{C_S})} \ll 1 \quad \Rightarrow \quad \frac{dv_p}{dt} \ll \frac{C_S^2}{2L} \quad (1)$$

Note that the upper bound for quasistatic ramp rate goes to zero for large systems. The advantage of the method is lost when systems are too large.

APPLICATION TO LENNARD-JONES

As a prelude to more realistic but computationally intensive studies, we test these ideas with the Lennard-Jones potential, which has a well-documented solid shock response [7] [3].

Simulation Details

We use the cubic-spline Lennard-Jones $6-12$ potential [8] in order to allow easy comparison with published Hugoniot results of Germann et al. [1]. The shock was oriented along the $<100>$ direction of the fcc crystal with unit cell dimension $5.314\ \text{Å} = 1.561\sigma$. Initial temperature was varied with a weak Langevin thermostat from zero to $10\text{K} =$

$0.083\,k_B\mathrm{T}/\varepsilon$. Results are found not to depend on the initial temperature for shock driving velocities, v_p above $0.75C_o$. Systems were 20×20 lattice planes in cross-section with transverse periodic boundary conditions. The timestep was 0.3 femtoseconds.

The traditional shock simulation runs (benchmark runs) were driven by a warm impactor and reached 600 Å in length ($\sim$100,000 particles). Continuous Hugoniot Method runs were held to 200 Å in length ($\sim$20,000 particles), at any one time. The cumulative distance covered by these treadmilling runs was almost 1.3 μm in length, and would have required over 1,200,000 particles in a conventional simulation. Every shock was given time to establish a steady state (usually 30 to 60 ps). The ramp rate of $0.001\,\mathrm{m/s}$ per step $= 3.3 \times 10^{12}\,\mathrm{m/s^2}$ is used for the remainder of this article. We report on our efforts in the strong shock regime, for driving velocities ranging from $v_p = 0.75C_o$ to $1.5C_o$.

Principal Hugoniot Results

The Continuous Hugoniot Method allows a system to move directly from one shock state to another. Therefore, the path of our Continuous Hugoniot Method through U_s–v_p space during a single run is the principal Hugoniot of final shock states in the material. This is true to the extent that there is quick convergence within the reduced system to the values far behind the shock. Figure 2 shows such a path for a simulation which runs from $v_p = 0.75C_o$ continuously through $v_p = 1.5C_o$. Initial and terminal benchmark runs, bookend the ramp. The Hugoniot fit proposed by Germann et al. is plotted in its applicable range.

We see excellent agreement of our method's results with both comparisons. In the lower range of v_p, where we can compare to the published fit, our data overlays the fit very nicely and continue it smoothly beyond the range for which it was originally published. At higher shock strengths our data stiffens (as it should), showing a super-linear increase in U_S vs v_p. In the upper range of v_p, we compare to our terminal benchmark results, which also agree well.

Comparison of Density Profiles

Figure 2 shows a series of four density profile snapshots taken from a continuous Hugoniot ramp (shown as solid lines). They are at $v_p = 0.75\,C_o$, $0.9\,C_o$, $1.2\,C_o$ and $1.5\,C_o$. The density profiles of the two benchmark runs and the final densities predicted by the Hugoniot fit for $0.75\,C_o$ and $0.9\,C_o$ are plotted.

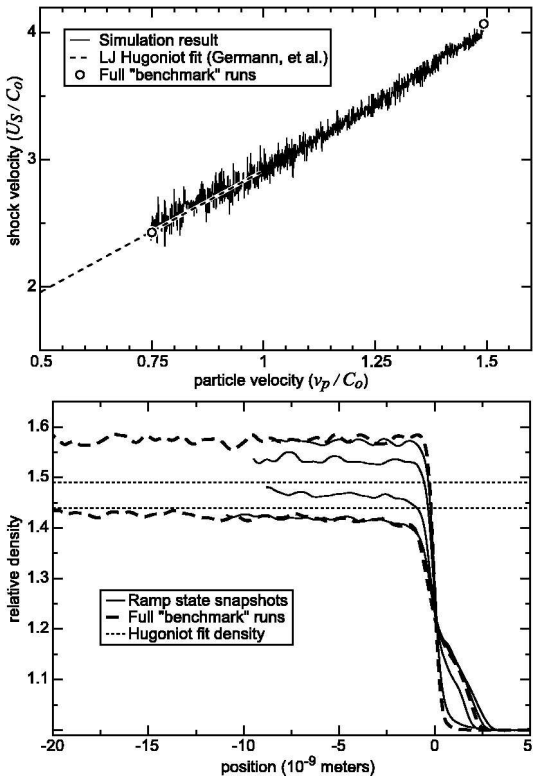

FIGURE 2. (top) Results of the Continuous Hugoniot Method, the fit of Germann et al. [1], and bookend benchmark runs. (bottom) Density profiles snapshots from a shock strength ramp (solid), from the initial and terminal benchmarks (dashed), and from the Hugoniot fit (dotted).

The profiles produced by the Continuous Hugoniot Method agree well with the results of the benchmark runs up to the point where they are purged. The benchmark densities, however, continue to grow beyond this point. In both cases the density predicted by the published fit is approximately 2% larger than the average final density produced by the Continuous Hugoniot Method. It appears that the density requires a larger spatial region than we have provided in order to converge completely to its asymptotic value.

Comparison of Final States

The final state of the Hugoniot ramp is a particularly important point of comparison because it is the state of the maximum integrated error. Figure 3 provides snapshots from the terminal benchmark (top) and the Continuous Hugoniot Method (bottom). The slices are along the x–z plane at the final piston velocity

$v_p = 1.5C_o$. Both systems exhibit a strong disordering transition on similar length scales, islands of incomplete disordering, and a common sharp density rise. Both have also developed forward-reaching features ahead of the front. Figure 3, shows very good agreement between the radial distribution functions for the material behind each front.

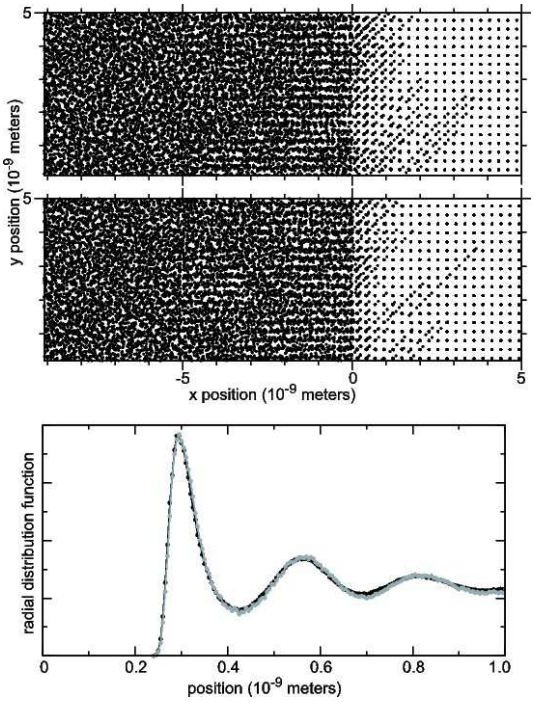

FIGURE 3. Structural dynamics and rdf comparison – Particle slices in the region of the shock front for states from (middle) the Continuous Hugoniot Method and (top) the terminal benchmark. Also shown (bottom) is a comparison of radial distribution functions for the compressed material extending 10 nm behind each front. $v_p = 1.5\,C_o$.

Efficiency and speed up

The computational speedup provided by the Continuous Hugoniot Method depends upon the density of points with which one wants to locate the Hugoniot. We find that the computation time to compute two benchmark runs by traditional methods is approximately equal to the computation time we employed to compute the entire intermediate Hugoniot, via our method. Thus if we had chosen to trace out the Hugoniot by interpolation with 10 conventional shock computations, we would have required 5 times more computation. More generally, let N_h be the number of traditional runs needed to map the Hugoniot between two states as a function of shock strength. Then the speed up is linear in N_h, given roughly by $N_h/2$. Alternatively, we point out we were able to simulate the cumulative effect of 1,280,000 particles with the resources required to hold only 20,000 at any one time.

CONCLUSIONS

We have presented the Continuous Hugoniot Method for efficient simulation of the dynamics in steady-state shock fronts. We confirmed in a Lennard-Jones system that the loading path of the Continuous Hugoniot Method followed the published Hugoniot fit. Comparison of particle snapshots and radial distribution functions at the final state of the Continuous Hugoniot Method ramp also showed good agreement with traditional shock methods.

All these measurements were made with greatly reduced computational expenditure over traditional methods. These savings are proving critical as the method is applied to more realistic and computationally costly potentials such as tin.

ACKNOWLEDGMENTS

We thank Todd Ditmire, Stephan Bless and Will Grigsby for useful conversations. This work was supported by the National Science Foundation under DMR-0401766, and DMR-0101030 and by the U.S. Dept. of Energy, National Nuclear Security Administration under Contract DE-FC52-03NA00156.

REFERENCES

1. Germann, T. C., et al., *Phys. Rev. Lett.*, **84**, 5351–5354 (2000).
2. Kadau, K., et al., *Int. J. of Modern Phys. C*, **15**, 193-201 (2004).
3. Holian, B. L., and Lomdahl, P. S., *Science*, **280**, 2085–2088 (1998).
4. Maillet, J. B., et al., *Phys. Rev. E*, **63**, 16121 (2000).
5. Reed, E. J., et al., *Phys. Rev. Lett.*, **90**, 235503 (2003).
6. Zhakhovskii, V. V., et al., *Phys. Rev. Lett.*, **83**, 1175–1178 (1999).
7. Holian, B. L., *Shock Waves*, **5**, 149–157 (1995).
8. Holian, B. L., et al., *Phys. Rev. A*, **43**, 2655–2661 (1991).